

Video Based Measurement of Heart Rate and Heart Rate Variability Spectrogram from Estimated Hemoglobin Information

Munenori Fukunishi, Kouki Kurita
Chiba University
1-33 Yayoi-cho, Inage-Ku, Chiba
263-8522, JAPAN
fukunishi.m@gmail.com

Shoji Yamamoto
Tokyo Metropolitan College
8-17-1 Minami-Senju, Arakawa,
Tokyo 116-0003, JAPAN

Norimichi Tsumura
Chiba University
1-33 Yayoi-cho, Inage-Ku, Chiba
263-8522, JAPAN
tsumura@faculty.chiba-u.jp

Abstract

In this paper, we propose an accurate remote observation of the heart rate (HR) and heart rate variability (HRV) based on extracted hemoglobin information which is based on detail skin optics model. We perform experiments to measure subjects at rest and under cognitive stress with the proposed method putting a polarized filter in front of camera to evaluate the principal of the framework. From the results of the experiments, the proposed method shows a high correlation with the electrocardiograph (ECG) which is assumed as the ground truth. We also evaluated the robustness against illumination change in simulation. We confirmed that the proposed method could obtain accurate BVP detection compared with other conventional methods since the proposed method eliminates the shading component through the process of the extraction of hemoglobin component.

1. Introduction

Remote measurement of heart rate (HR) and heart rate variability spectrogram (HRVS) are active research area since these have great potential for health-care applications, medical applications and affective computing. The remote measurements of HR and HRVS, which have been proposed so far, can be roughly classified into two methods; active methods and passive methods.

Active methods utilize physical signals such as electromagnetic wave, microwave/millimeter-wave, or laser (speckle imaging). The HR detection based on electromagnetic wave utilizes a Doppler radar [1, 2, 3, 4]. The surface of human body is slightly moving by heartbeat. The technique detects the target's subtle movement by analyzing the phase shift caused by Doppler Effect. This approach is basically used only for the measurement of heart rate. The methods using microwave or millimeter-wave also utilize a Doppler radar for the detection of target's slight movement caused by heartbeat [5, 6]. The heartbeat detection by laser is based on so-called speckle imaging or laser speckle imaging. This method records the temporal fluctuations of light intensity

on the surface of skin by using visual camera [7]. Active methods are, in general, not so robust against subject movement since physical signals have to be projected on the same position of the subject.

Passive method is a method to monitor heartbeat by using visual camera. Skin color also slightly changes periodically due to the heartbeat. According as the advance of sensor technology, it has become possible to detect such subtle color change. Takano and Ohta proposed a new device combining a time-lapse image by a handy video camera and image processing on a PC, and found that it could measure the 30s average heart rate and respiratory rate based on the changes in the brightness of the ROI set around the cheek of the unrestricted subject [8]. The measurements were successfully conducted for the subjects with or without facial cosmetics. Verkrusse *et al.* demonstrated the measurement of BVP under ambient light using the G channel of movies captured by a consumer camera [9]. One of the epoch making application of image-based techniques is the "cardiocam" as it has been named by its authors, Poh *et al.* which is a low-cost technology for measurement of heart rate using a cheap digital imaging device such as a webcam [10, 11]. The method extracted pulse wave from time series signal of R, G and B average value in region of interest (ROI) by utilizing blind source separation. Another image-based system has been developed by Philips Research Laboratory. A prototype for heart rate monitoring with a small battery and camera has been realized and demonstrated on professional swimmers for unrestrained heart rate measurement [12]. Haan *et al.* proposed a remote photoplethysmography (rPPG) measurement which is based on simple skin reflection model [13, 14, 15, 16]. They showed that rPPG could monitor subject's heartrate robustly even when the subject was during exercising. The method extract intensity component, specular component, pulse component from input RGB video frames.

Heart rate variability spectrograms (HRVS) are useful for non-invasive monitoring of the autonomic nervous system, which controls involuntary body functions, such as breathing, blood pressure, and heartbeat. The low-frequency (LF) power in HRVS (0.05-0.15 Hz) is widely known as one of the most reliable indicators of sympathetic activity since the power increases under

cognitive stress [17]. The high frequency (HF) power in HRVS (0.15-0.40 Hz) is affected by breathing and is related to parasympathetic activity. McDuff et al. [18] developed a remote HRVS measurement technique using a special sensor with five color channels (16 bits/channel): red, green, blue, cyan, and orange (RGBCO) [19, 20]. They showed the effectiveness of their HRVS measurement for observation of the nervous system activity both under the condition at rest and under cognitive stress respectively. However, those technologies are still under research phase or demonstration phase by prototype. For further practical use, more robust technology is required.

On another front, estimation methods for skin components have been proposed based on skin optics. Tsumura *et al.* [21] proposed a method for estimating hemoglobin, melanin, and shading components from a skin color image. The detail skin optics model has a potential to enhance the robustness against environmental change for remote HR and HRVS monitoring because it is known that skin reflection model is useful to enhance the robustness as proposed in rPPG [13]. Hence, we proposed a non-contact video based monitoring method for heart rate and heart rate variability spectrograms by utilizing detail skin optics framework [22] However, in the previous paper, we did not perform the evaluation of robustness for environmental changes.

In this paper, therefore, we report the extended version of the previous paper on the aspect of the evaluation of robustness for environmental changes. The rest of this paper is organized as follows. In Section 2, we outline the method for extracting hemoglobin information from skin images which was already introduced in our previous paper.. In Section 3, we adapt the method from Section 2 to measure BVP and HRVS by adding detail analysis compared with our previous research. In Section 4, we describe the experimental setup and show the results of BVP detection with the proposed method, and compare them with ECG data as the ground truth and with the conventional method using a five-band camera. We also show experimental results from stress monitoring. In Section 5, we present our conclusions.

2. Extraction of Hemoglobin Information from Skin Image

Estimation methods for skin components have been proposed by Tsumura *et al.* [21]. The method estimate hemoglobin, melanin, and shading components based on skin optics from a skin image captured by a standard RGB camera. In this section, we describe the skin model and the way to estimate the skin component.

Figure 1 shows the skin model for the extraction of hemoglobin component. The model is two-layered skin model composed of epidermis and dermis. We simplify the model assuming that epidermis and dermis only have

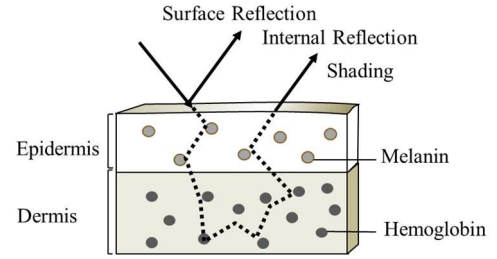


Figure 1: Skin Model for the Estimation of Hemoglobin, Melanin, Shading [21]

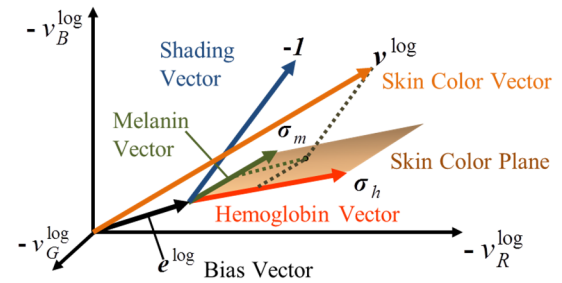


Figure 2: Skin Color Vector and Melanin, Hemoglobin and Shading Vectors [21]

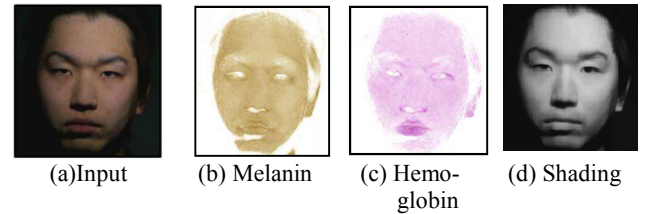


Figure 3: Estimation Results of Melanin, Hemoglobin and Shading Component

chromophores of melanin and hemoglobin respectively. The light from the skin surface consists of surface reflection and internal reflection. The modified Lambert-Beer law [23] is used to describe the behavior of internal reflection. The spectral radiance $L(x, y, \lambda)$ at the position (x, y) on the surface is described by

$$L(x, y, \lambda) = e^{-\rho_m(x,y)\sigma_m(\lambda)l_s(\lambda) - \rho_h(x,y)\sigma_h(\lambda)l_d(\lambda)} E(x, y, \lambda), \quad (1)$$

where λ is the wavelength, $E(x, y, \lambda)$ denotes the spectral irradiance of incident light at point (x, y) , and $\rho_m(x, y)$, $\rho_h(x, y)$, and $\sigma_m(\lambda)$, $\sigma_h(\lambda)$ are the densities of the chromophores and the spectral cross-sections of the melanin and hemoglobin, $l_s(\lambda)$, $l_d(\lambda)$ denote the mean path lengths of photons in the epidermis and dermis layers, respectively. Polarization filters are put in front of the illumination and camera in the position as crossed nicols when we simplify the behavior by ignoring the surface reflection.

Camera signal $v_i(x, y)$, $i = R, G, B$ can be modeled as

$$\begin{aligned}
v_i(x, y) &= k \int L(x, y, \lambda) s_i(\lambda) d\lambda \\
&= k \int e^{-\rho_m(x, y) \sigma_m(\lambda) l_e(\lambda) - \rho_h(x, y) \sigma_h(\lambda) l_d(\lambda)} E(x, y, \lambda) s_i(\lambda) d\lambda \\
&\quad (i = R, G, B) \tag{2}
\end{aligned}$$

where $s_i(\lambda)$ denotes the spectral sensitivity of a camera, and k denotes the coefficient of camera gain. Since the spectral reflectance curve of skin is smooth and roughly correlated with camera sensitivity, we can approximately assume $s_i(\lambda) \approx \delta(\lambda - \lambda_i)$. We assume the spectral irradiance of incident light $E(\lambda)$ can be written as the following equation.

$$E(x, y, \lambda) = p(x, y) \bar{E}(\lambda). \tag{3}$$

Here, the factor $p(x, y)$ is related to shading information and $\bar{E}(\lambda)$ indicates that the basic color of illumination is the same at any point on the surface of the object. The camera signal can be rewritten as

$$v_i(x, y) = k e^{-\rho_m(x, y) \sigma_m(\lambda_i) l_e(\lambda_i) - \rho_h(x, y) \sigma_h(\lambda_i) l_d(\lambda_i)} p(x, y) \bar{E}(\lambda_i) \tag{4}$$

By taking the logarithm of both sides of Equation (4), we can derive the following equation.

$$\mathbf{v}^{log}(x, y) = -\rho_m(x, y) \boldsymbol{\sigma}_m - \rho_h(x, y) \boldsymbol{\sigma}_h + p^{log}(x, y) \mathbf{1} + \mathbf{e}^{log}$$

where

$$\begin{aligned}
\mathbf{v}^{log}(x, y) &= [\log(v_R(x, y)) \quad \log(v_G(x, y)) \quad \log(v_B(x, y))]^T \\
\boldsymbol{\sigma}_m &= [\sigma_m(\lambda_R) l_e(\lambda_R) \quad \sigma_m(\lambda_G) l_e(\lambda_G) \quad \sigma_m(\lambda_B) l_e(\lambda_B)]^T \\
\boldsymbol{\sigma}_h &= [\sigma_h(\lambda_R) l_d(\lambda_R) \quad \sigma_h(\lambda_G) l_d(\lambda_G) \quad \sigma_h(\lambda_B) l_d(\lambda_B)]^T \\
\mathbf{1} &= [1 \quad 1 \quad 1]^T \\
p^{log}(x, y) &= \log(p(x, y)) + \log(k) \\
\mathbf{e}^{log}(x, y) &= [\log(E_R(\lambda_R)) \quad \log(E_G(\lambda_G)) \quad \log(E_B(\lambda_B))]^T \tag{5}
\end{aligned}$$

Therefore, the logarithm of the captured RGB signals \mathbf{v}^{log} can be represented by the weighted linear combination of the three vectors $\boldsymbol{\sigma}_m$, $\boldsymbol{\sigma}_h$ and $\mathbf{1}$ with the bias vector \mathbf{e}^{log} as shown in Figure 2. We predefine a skin color plane using training data set. The logarithm of the captured RGB signals \mathbf{v}^{log} is projected onto the skin color plane along with the shading vector $\mathbf{1}$. From the position on the skin plane, we obtain the hemoglobin vector $\boldsymbol{\sigma}_h$.

Figure 3 provides the estimation results for the melanin, hemoglobin, and shading components from the input image. We can see the mole and pigmented spot in the melanin component and pimples in the hemoglobin component. The shading image provides a reasonable representation of the facial structure.

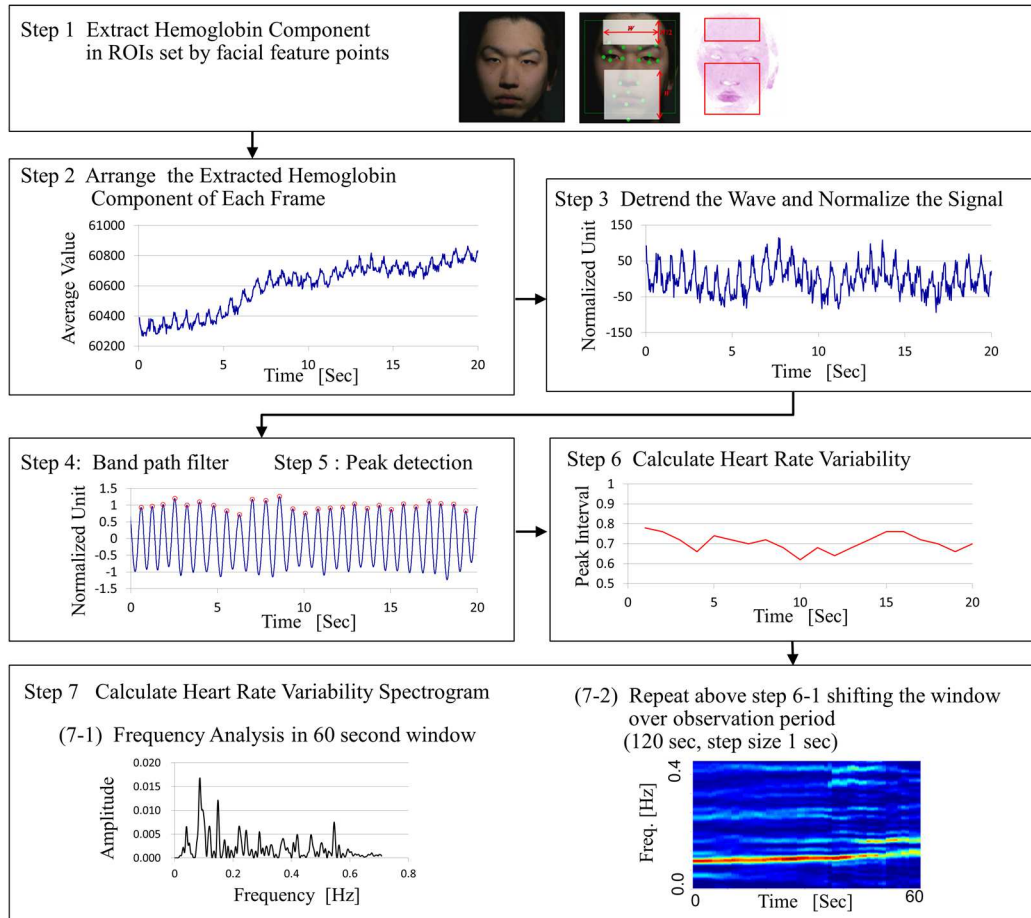


Figure 4: Signal Processing to Detect Blood Volume Pulse and Heart Rate Variability Spectrogram [22]

3. BVP Measurement using Hemoglobin Information

In this section, we describe the procedure for obtaining the BVP and HRVS based on the extracted hemoglobin information. Figure 4 shows the procedure of the signal processing for the detection of BVP and HRVS. In Step 1, we extract the hemoglobin component in each frame from the facial capture video. The regions of interest (ROIs) are set based on the facial landmarks detected by LEAR [24] in order to compensate for the face movement. In Step 2, we form the wave of hemoglobin component. The moving average of the waveform changes with time in some case because of the facial movement. In Step 3, detrending technique [25] is applied for the waveform to eliminate the temporal variations of the moving average. In Step 4, a band-pass filter is applied for the waveform to extract the heart beat components. The property of the band-pass filter is decided based on the pace of heartbeat, which have a frequency between 0.75 Hz (45 beats-per-minute) and 3 Hz (180 beats-per-minute). In Step 4, the local peaks of the BVP waveform are detected. The red circles on the BVP waveform indicate peaks of heartbeat. In Step 6, the time intervals of each peak are calculated by subtracting the peak time from the previous timing and form the waveform of heart rate variability (HRV). In step 7, Lomb-Scargle periodograms [26, 27] is calculated using the waveform of HRV and the frequency property is obtained in each second by shifting the 60-second window over the 120-second sampling period.

Figure 5 shows examples of the HRV spectrograms obtained by the above method. At rest, the parasympathetic nerve is activated. The parasympathetic nerve is influenced by the activity of respiratory sinus arrhythmia (RSA). Since usual breathing rate is between 10 and 25 inhalations per minute, the HF (0.15-0.4 Hz) power spectrum is increased at rest. On the other hand, under cognitive stress, the sympathetic nerve is activated. The sympathetic nerve is related to fluctuations in the blood pressure and it can

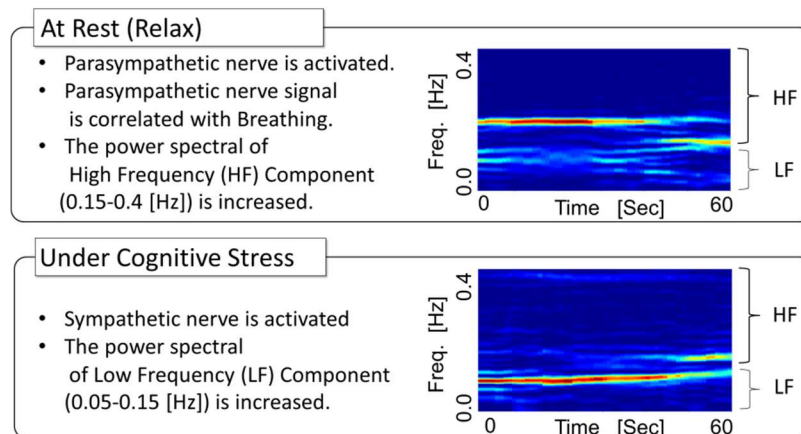


Figure 5: Relationship between the sympathetic nervous system and Heart Rate Variability Spectrogram

transmit only very low frequency signals. Hence, the LF (0.04-0.15 Hz) powers were modulated under cognitive stress. By observing the HF and LF components, we can estimate the subject's stress levels.

4. Experiment

4.1. Experimental Setup

Figure 6 shows the experimental setup used to obtain the BVP and HRVS with our method. The video data of a subject's face were taken from a distance of 3 meters with a digital single-lens reflex (DSLR) camera with a sensor of the five color (i.e., RGBCO) channels (12 bits/channel) [6]. We use the data of RGB channels to evaluate the proposed method, the Independent Component Analysis (ICA) based method [4] and chrominance based rPPG [7]. We also use the data of RGBCO channels for Independent Component Analysis (ICA) based method [4]. The frame rate of the camera was 30 frames per second (fps). Each frame was 640×480 pixels. A standard Zuiko 50 mm lens was used in our experiment. Each frame was saved on a laptop PC (Dell Inc. Latitude E6530, 2.4 GHz, 3 MB cache). Artificial solar light (SERIC Ltd. SOLAX XC-100) was used to illuminate the face at a distance of 0.5 m from the subject. We put polarized filters (crossed nicols) in front of the source of illumination and camera to simplify the estimation of the hemoglobin component by removing surface reflection. The measurements taken with the electrocardiograph (NIHON KOHDEN RMT-1000) were used for the ground truth. In the experiments, we obtained videos from 4 participants. The subjects were three Japanese males and one female aged from 21 to 48 years old. The experiments for each subject were conducted under the two conditions, at rest (not under cognitive stress) and under cognitive stress (The subjects were required to keep subtracting 7 from 4000) respectively. The duration is 120 second and the window size of spectral analysis is 60 seconds.

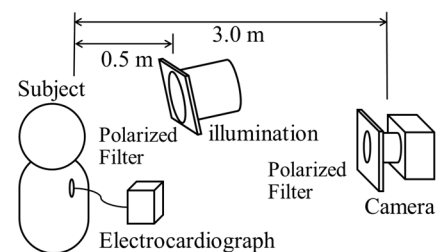


Figure 6: Experimental Setup

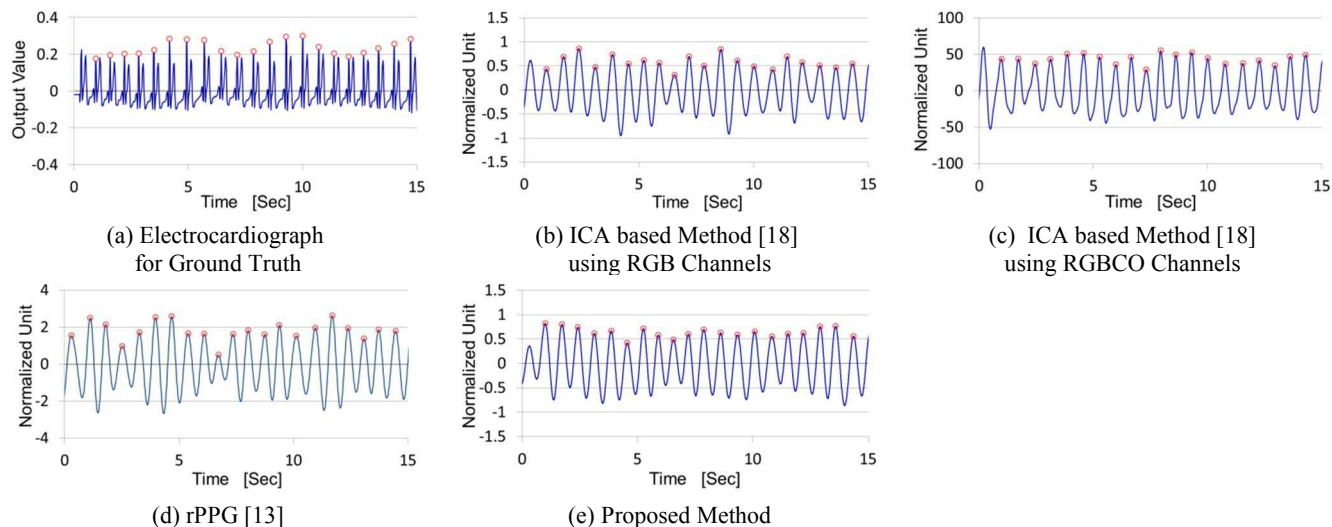


Figure 7: Results of Blood Volume Pulse (BVP) Detection and Electrocardiograph Data for Ground Truth

Table 1: Accuracy of the Measured Heart Rates at Rest and under Cognitive Stress

		(a) Relax				(b) Cognitive Stress			
		Subject #1	Subject #2	Subject #3	Subject #4	Subject #1	Subject #2	Subject #3	Subject #4
Heart Rate [bpm] *beat per minute	Electrocardiogram	83.63	64.40	60.78	72.75	84.61	71.82	60.97	72.19
	ICA based [18] w/ RGB	83.28	63.81	61.16	73.02	84.26	71.23	61.39	72.02
	ICA based [18] w/ RGBCO	83.43	63.85	61.04	72.99	84.38	72.10	61.31	72.10
	rPPG [13]	83.58	63.85	61.17	77.92	84.01	71.30	61.39	72.08
	Proposed method	83.50	63.87	60.08	72.81	84.74	72.06	61.30	72.15
Accuracy [%]	ICA based [18] w/ RGB	99.58	99.08	99.37	99.63	99.59	99.18	99.31	99.76
	ICA based [18] w/ RGBCO	99.76	99.15	99.57	99.67	99.73	99.61	99.44	99.88
	rPPG [13]	99.94	99.15	99.36	92.89	99.29	99.28	99.31	99.85
	Proposed method	99.84	99.18	98.85	99.92	99.85	99.67	99.46	99.94

4.2. Experimental Results

Figure 7 shows the electrocardiogram (ECG) as ground truth and the results of remote BVP detected by 4 methods: independent component analysis (ICA) based method [18] using RGB channels, ICA based method [18] using RGBCO channels, chrominance based rPPG [13] using RGB channels, and the proposed method based on the extracted hemoglobin information using RGB channels. The red circles indicate local peaks of the BVP. The ECG data has two peaks in each pulse interval. I put red circle on the first peak as the local peak for the each heartbeat. Each BVP wave has 20 or 21 peaks, red circle; these detections work properly.

Tables 1 show the heart rate (HR) detection for 4 subjects at rest and under cognitive stress respectively. The HR is obtained by the following equation.

$$heart\ rate = 60 / \overline{peak\ interval}$$

Here, $\overline{peak\ interval}$ is the average of the time intervals of each peak. The figures in Tables 1 also show the accuracy of HR comparing with ECG data. The results show that the proposed method, ICA based method [18] and rPPG [13] can obtain around 99% accuracy of HR and there is no big difference with respect to the performance of HR. detection. Figure 8 shows the results of the HRVS of Subject 1. Each spectrogram is described in heat map format. Red indicates high powers, and blue indicates low power. Each results under cognitive stress shows high power of LF (0.04-0.15 Hz); each results at rest shows high power of HF (0.15-0.4 Hz). These features agree with a prior study on sympathetic activity [16]. In detail, the conventional methods, ICA based method with RGB, RGBCO and rPPG, show somewhat high power in HF

(0.15-0.4 Hz) region even when subject is under cognitive stress. On the other hand, the proposed method does not show high power in HF region and it well agrees with the result of ground truth. The results at rest also show that the proposed method better agree with the ground truth than the conventional methods. Figure 9 shows the example

of the detail analysis of inter-beat intervals as the input of HRVS. The blue lines in each graphs indicate the ground truth of inter-beat intervals; the red lines shows the inter-beat interval detected by ICA based method using RGB, RGBCO and the proposed method respectively. The proposed method well agrees with the ground truth

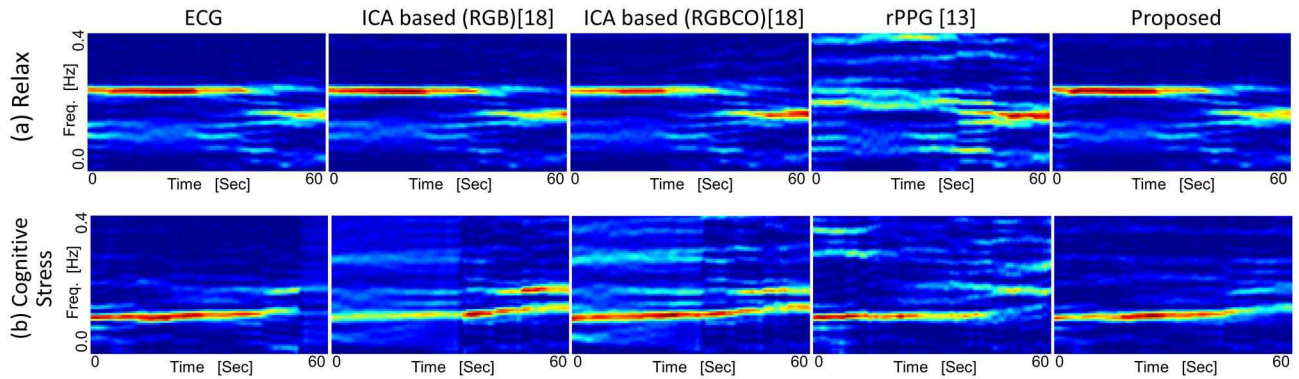
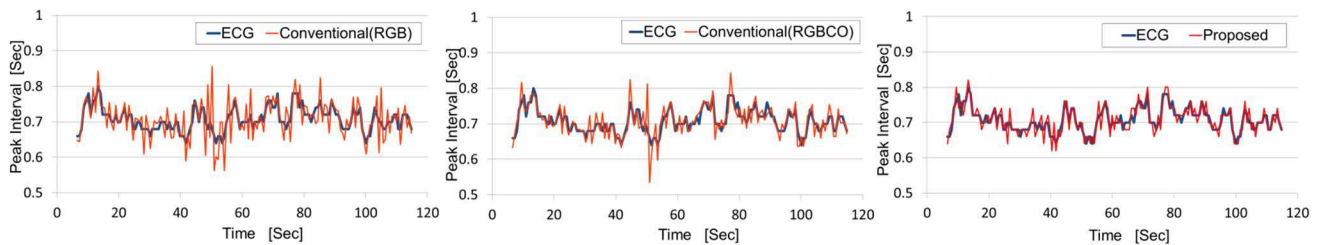


Figure 8: Heart Rate Variability Spectrograms



(a) Electrocardiograph for Ground Truth

(b) ICA based Method [18] using RGB Channels

(c) ICA based Method [18] using RGBCO Channels

Figure 9: Examples of the inter-beat intervals as the input of HRVS (Subject 1, under cognitive stress)

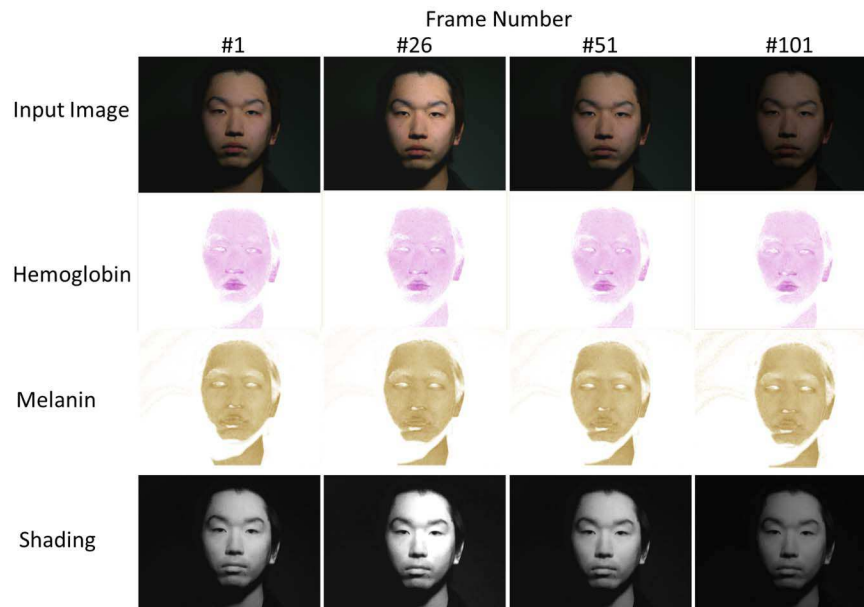


Figure 10: Input Images and the separations (Hemoglobin, Melanin, Shading) under the condition of illumination change. Shading image show the effect from the illumination change, whereas the hemoglobin and melanin images do not show the effect from the illumination change respectively.

apparently. That is, the proposed method can obtain more accurate detection of HR comparing with existing method.

We also evaluated the robustness against illumination change. For this experiment, we simulated the illumination change for the input images and evaluate BVP detection. Figure 10 shows the input images and the separations under the condition putting illumination change. The shading components are influenced by the illumination change. On the other hand, hemoglobin components and melanin components do not show any clear effect from the illumination change. Figure 11 shows the results of BVP detection under the condition of illumination change. Table 2 indicates the difference of peak timing of BVP between without illumination change and with illumination change. The proposed method has peak timing error of 0.0084 seconds. This is less than 0.0272 seconds for ICA based method using RGB, 0.0240 seconds for the ICA based using RGBCO and 0.1590 seconds for rPPG respectively. The proposed method eliminates the shading component

through the process of the extraction of hemoglobin component. Therefore, the proposed method can enhance the robustness against illumination change.

5. Conclusion

We report the extended version from previous paper [22] on a video based measurement of HR and HRVS based on the hemoglobin component extracted from each RGB input frames. Especially, in this paper, we evaluated the robustness against illumination change in simulation and we confirmed that the proposed method could obtain accurate BVP detection compared with other conventional methods since the proposed method eliminates the shading component through the process of the extraction of hemoglobin component.

At last we mention the limitation and the future work. Our experiment was conducted in an environment with no large motions of the subjects. It is necessary to evaluate the

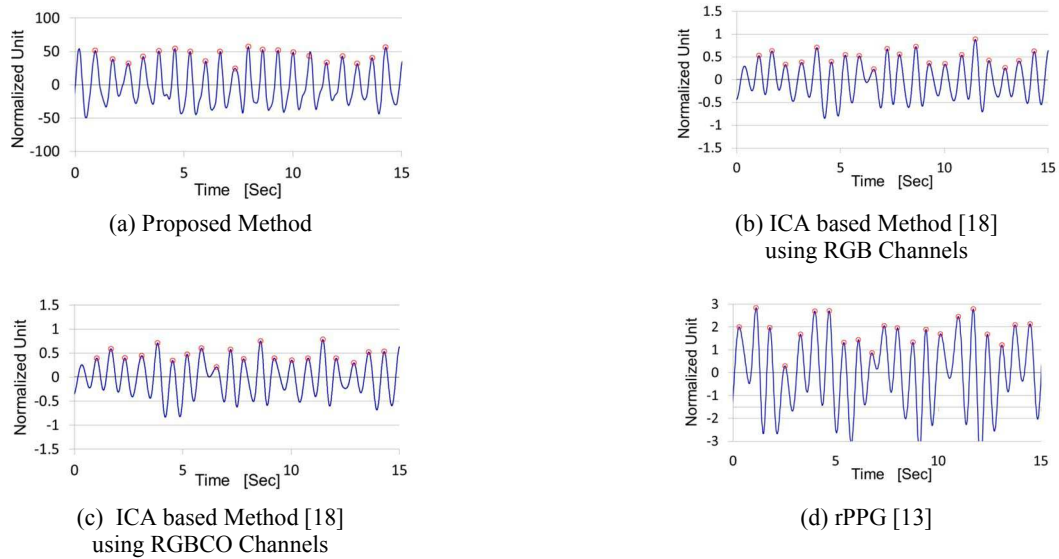


Figure 11: Results of Blood Volume Pulse (BVP) Detection under the condition of illumination change. (a) Proposed Method, (b) ICA based Method [18] using RGB Channels, (c) ICA based Method [18] using RGBCO Channels, (d) rPPG [13].

Table 2: The Average and the Standard Deviation of Peak Timing Between with and without Illumination Change

	(a) Proposed Method	(b) ICA based [18], RGB Channels	(c) ICA based [18], RGBCO Channels	(d) rPPG [13]
Average Error	0.0084 [sec]	0.0272 [sec]	0.0240 [sec]	0.1590 [sec]
Standard Deviation of Error.	0.0162 [sec]	0.0239 [sec]	0.0191 [sec]	0.2991 [sec]

method more under various conditions. We evaluated only Asian subjects in the experiment. We have to confirm the effectiveness of the skin component extraction for another skin type as well.

References

- [1] Y. Xiao, J. Lin, O. Boric-Lubecke, V.M. Lubecke, "Frequency-tuning technique for remote detection of heartbeat and respiration using low-power double-sideband transmission in the ka-band", *IEEE Trans. Microw. Theory Tech.*, vol. 54, no. 5, pp. 2023-2032, (2006).
- [2] C. Li, J. Lin; "Random body movement cancellation in Doppler radar vital sign detection", *IEEE Trans. Microw. Theory Techn.*, vol. 56, no. 12, pp. 3143-3152, (2008).
- [3] D. Obeid, S. Sadek, G. Zaharia, G. El Zein, "Touch-less heartbeat detection and cardiopulmonary modeling", *Proc. 2nd Int. Symp. Appl. Sci. Biomed. Commun. Technol. (ISABEL)*, pp. 1-5, (2009).
- [4] D. Nagae, A. Mase, "Measurement of vital signal by microwave reflectometry and application to stress evaluation, " in *Proc. Asia Pacific Microwave Conference 2009 (APMC 2009)*, pp.477-480 (2009).
- [5] N. Tateishi, A. Mase, L. Bruskin, Y. Kogi, N. Ito, T. Shirakata, and S. Yoshida, "Microwave measurement of heart beat and analysis using wavelet transform", *Proc. Asia Pacific Microwave Conf., Bangkok*, pp. 2151-2153. Dec. (2007).
- [6] D. Nagae, A. Mase; Measurement of heart rate variability and stress evaluation by using microwave reflectometric vital signal sensing. *Rev Sci Instrum* 81, 094301.(2010).
- [7] Da Costa, Optical remote sensing of heartbeats. *Optics Communications*, 117(5-6):395-98 (1995).
- [8] Takano, C., and Ohta, Y., Heart rate measurement based on a time-lapse image. *Med. Eng. Phys.* 29(8):853-857, (2007).
- [9] W. Verkruysse, L. O. Svaasand and J. S. Nelson, "Remote plethysmographic imaging using ambient light," *Opt. Exp.*, vol. 16, no. 26, pp. 21434-21445, (2008).
- [10] M.-Z. Poh, D. J. McDuff, and R. W. Picard, "Non-contact, automated cardiac pulse measurements using video imaging and blind source separation," *Optics Express*, vol. 18, no. 10, pp. 10 762-10 774, (2010).
- [11] M-Z. Poh, D. McDuff, R.W. Picard. "Advancements in noncontact, multiparameter physi-ological measurements using a webcam." *IEEE Transactions on Biomedical Engineering* vol.58, no.1, pp.7-11 (2011).
- [12] Van Rooijen V, de Voogd-Claessen L, Lauche K, Jeanne V, van der Vliet R; Development of a new product for unrestrained heart rate measurement in swimming: a user centered design approach. *Procedia Engineering* , vol. 2, no. 2, pp. 2693-2699 (2010).
- [13] G. De Haan, V. Jeanne. "Robust pulse rate from chrominance-based rPPG," *IEEE Transactions on Biomedical Engineering*, vol. 60, no. 10, pp. 2878-2886 (2013).
- [14] G. de Haan and A. van Leest, "Improved motion robustness of remote-PPG by using the blood volume pulse signature," *Physiological Measurement*, vol. 35, no. 9, pp. 1913-1922, Oct. (2014).
- [15] W. Wang, S. Stuijk, and G. de Haan, "A novel algorithm for remote photoplethysmography: Spatial subspace rotation," *Biomedical Engineering, IEEE Transactions on*, vol. PP, no. 99, pp. 1-1, (2015).
- [16] W. Wang, A. den Brinker, S. Stuijk, and G. de Haan, "Algorithmic principles of remote PPG", *IEEE Trans. Biomed. Eng.*, vol. 64, no. 7, pp. 14791491, Jul. (2016).
- [17] Pagani M, Furlan R, Pizzinelli P, Crivellaro W, Cerutti S, Malliani A. Spectral analysis of R-R and arterial pressure variabilities to assess sympatho-vagal interaction during mental stress in humans. *J Hypertens*; 7 (Suppl): S14-5, (1989).
- [18] D. McDuff, S. Gontarek, R. W. Picard, "Improvements in Remote Cardio-Pulmonary Measurement Using a Five Band Digital Camera" *IEEE Transactions on Biomedical Engineering*, pp. 2593-2601, (2014).
- [19] Y. Monno, M. Tanaka, and M. Okutomi, "Multispectral demosaicking using guided filter," in *IS&T/SPIE Electronic Imaging. International Society for Optics and Photonics*, pp. 82 9900-82 9900 (2012).
- [20] Y. Monno, S.Kikuchi, M. Tanaka, and M. Okutomi, "A Practical One-Shot Multispectral Imaging System Using a Single Image Sensor", *IEEE Trans. Image Processing*, vol.24, no.10, pp.3048-3059, Oct. (2015).
- [21] N. Tsumura, N. Ojima, K. Sato, M. Shiraishi, H. Shimizu, H. Nabeshima, S. Akazaki, K. Hori, Y. Miyake, "Image-based skin color and texture analysis/synthesis by extracting hemoglobin and melanin information in the skin," *ACM Trans. on Graphics*, Vol.22, No.3, 770-779, (2003).
- [22] Munenori Fukunishi, Kouki Kurita, Shoji Yamamoto, Norimichi Tsumura, "Non-contact video-based estimation of heart rate variability spectrogram from hemoglobin composition" *Artificial Life and Robotics*, Vol.22, Issue 4, pp 457-463, Dec.(2017).
- [23] M.Hiroka, Firbank M., Essenpreis M., Cope M., Arrige S. R., Zee P. V. D., Delpy D. T., "A Monte Carlo investigation of optical pathlength in inhomogeneous tissue and its application to near-infrared spectroscopy." *Phys. Med. Biol.* 38, 1859-1876. (1993).
- [24] B. Martinez, M. F. Valstar, X. Binefa and M. Pantic "Local evidence aggregation for regression-based facial point detection",*IEEE Trans. Pattern Anal. Mach. Intell.*, vol. 35, no. 5, pp. 1149-1163, May, (2013).
- [25] M. P. Tarvainen, P. O. Ranta-aho and P. A. Karjalainen "An advanced detrending method with application to HRV analysis", *IEEE Trans. Biomed. Eng.*, vol. 49, no. 2, pp. 172-175, Feb., (2002).
- [26] Scargle, J. D. Studies in astronomical time series analysis. II - Statistical aspects of spectral analysis of unevenly spaced data. *ApJ* 1:263 pp. 835-853 (1982)
- [27] Press, William H., and George B. Rybicki. "Fast Algorithm for Spectral Analysis of Unevenly Sampled Data", *Astrophysical Journal*. Vol. 338, pp. 277-280.(1989)